Pentachlorocyclopropane/Base Complexes: Matrix Isolation Infrared Spectroscopic and Density Functional Study of C−H- - -N Hydrogen Bonds

Alexander B. Baker and Cindy Samet*

Department of Chemistry, Dickinson College, Carlisle, Pennsylvania 17013

Jonathan T. Lyon and Lester Andrews

Department of Chemistry, University of Virginia, P.O. Box 400319, Charlottesville, Virginia 22904-4319

Received: June 1, 2005; In Final Form: July 26, 2005

Hydrogen-bonded complexes of pentachlorocyclopropane with the bases acetonitrile, ammonia, monomethylamine, and dimethylamine have been isolated and characterized for the first time in argon matrices at 16 K. Coordination of the proton of pentachlorocyclopropane (Pccp) to the electron donor (N) of the base was evidenced by red shifts of the CH stretching mode. These shifts, which range from 22 to 170 cm^{-1}, increase in the order CH_3CN, NH_3, $(CH_3)NH_2$, and $(CH_3)_2NH$. Density functional theory (DFT) calculations at the B3LYP level agree well with experiment and support the formation of 1:1 complexes of Pccp/base. Distinct changes were observed in ring modes as well as CCl and CCl_2 modes. The hydrogen bond energy of the complexes varies from 2.95 to 4.22 kcal/mol and is stronger than our previously studied bromocyclopropane−ammonia complex (2.35 kcal/mol, MP2).

Introduction

Hydrogen bonds involving the C−H group, although documented as early as 1960,[1] elude undergraduate chemistry textbooks and are rarely mentioned in the curriculum at all. In 1982, the first crystallographic evidence of C−H- - -X hydrogen bonds was published,[2] and since then, studies involving C−H- - -O and C−H- - -N hydrogen bonds have been prolific.[3] These "nontraditional" hydrogen bonds do not fit the textbook definition of a hydrogen bond being an interaction of a partially positive charged proton situated between two highly electronegative atoms such as N, O, or F. It has been found that these weak interactions play important roles in chemistry and biology, including such areas as molecular recognition,[4] crystal engineering,[5] and the structure and stability of biomolecules.[3] C−H- - -O hydrogen bonds have been studied extensively,[6] especially with regard to the role of C_α−H- - -O in stabilizing protein structures.[7] C−H- - -N hydrogen bonds, however, have not been studied to the same extent experimentally, although there are numerous published studies,[8] including one that describes the importance of the C−H- - -N hydrogen bond on the coordination structure of manganese(III)−porphyrin complexes.[9] In addition, they have been the subject of numerous theoretical investigations,[10] including one that demonstrates they are significant in RNA base pairing.[11]

Previously in our laboratory, we formed complexes between bromocyclopropane (BrCp) and the nitrogen bases ammonia and trimethyamine. The resulting C−H- - -N hydrogen bonds that result are some of the weakest formed in a matrix to date and represent the first complexes in which a cyclopropane is shown to donate a proton in hydrogen bond formation.[12] Prior to our study, Legon[13] and Ault[14] showed that cyclopropane behaves as a proton acceptor, with hydrogen bonds forming to the electron-rich edge of the ring. Another study from our lab involving cyclopentadiene with N and O bases presents the first example of an sp^3-hybridized carbon that is not adjacent to a carbonyl (i.e., a non-α-carbon) or other electron-withdrawing substituents taking part in a C−H- - -N(O) hydrogen bond.[15]

This study builds on previous work and provides an interesting comparison with bromocyclopropane. For years, cyclopropane and its derivatives have been of interest to chemists. This small ring system occurs in a large number of organic natural products and steroids, including gorgosterol, which has been isolated from sea creatures. Halogenated derivatives have been used as anesthetics, pesticides, and fungicides.[16] Cyclopropane, c-C_3H_6, exhibits unusual chemical properties because of the high degree of ring strain and behaves more like an olefin than an alkane.[17,18] It is generally known that C−H bonds with high s-character exhibit exceptional acidity, and this explains the relatively high acidity of the C−H groups of cyclopropane.[19] Furthermore, adding electron-withdrawing substituents makes the proton even more acidic and strengthens the C−H- - -X hydrogen bond.[20] Pentachlorocyclopropane (Pccp) represents a novel molecule to study in that it is essentially the molecular "inverse" of a monosubstituted cyclopropane like BrCp, having five substituents and one hydrogen atom instead of five hydrogens and one substituent. This work therefore yields valuable comparative data on the C−H- - -N hydrogen bond.

Experimental and Computational Methods

All of the experiments conducted in this study were carried out in a completely stainless steel vacuum system, with Nupro Teflon-seat high-vacuum valves. Pumping was provided by a model 1400B Welch vacuum pump and either a Varian HSA diffusion pump with a liquid nitrogen trap or a turbomolecular pump (Varian V301). Vacuums on the order of 10^{-7} mmHg at the gauge (cold cathode, Varian) were attained using this apparatus. Cryogenics were supplied by a model 22 closed cycle helium refrigerator (CTI, Inc.), which operates down to 10 K. Gas samples were deposited from 2 L stainless steel vessels

10.1021/jp0581781 CCC: $30.25
Published on Web 08/30/2005

through a precise metering valve onto the cold surface, which is a CsI window mounted with indium gaskets to a copper block which is in turn mounted with indium gaskets on the second stage of the CTI Cryogenics refrigerator's cold head. Deposition of the gas samples was perpendicular to the cold surface. Temperatures at the second stage of the cold head were controlled and monitored by a LakeShore 321 digital cryogenic temperature controller. The vacuum vessel was equipped with CsI windows and sat in the sample beam of a Nicolet Nexus 670 infrared spectrometer for the duration of the experiment, and the sample was monitored during the entire deposition. The matrix isolation apparatus described here is standard and has been described thoroughly elsewhere in the literature.[21]

The gaseous reagents employed were CH_3CN, NH_3, $(CH_3)NH_2$, $(CH_3)_2NH$, and $(CH_3)_3N$ (all Matheson). These reagents were subjected to one or more freeze−thaw cycles at 77 K prior to sample preparation. Pccp (Acros Organics) was used without further purification. Argon (Matheson, 99.999%) was used without further purification as the matrix gas in all experiments.

Samples were deposited in the twin-jet mode (i.e., the two reactants were codeposited from separate vacuum lines). Because Pccp is relatively involatile, we attached a sidearm to the deposition line, separated by a valve. The argon then entrained the Pccp vapor from the sidearm. This technique is commonly used with samples whose vapor pressure is less than 1 mmHg at room temperature. The drawback to such a technique is that it is difficult to vary and measure matrix ratios. Samples were deposited at rates ranging from approximately 0.5 to 2 mmol/h, for times ranging from 22 to 30 h, and at temperatures ranging from 10 to 20 K. Survey scans and high-resolution scans were recorded at resolutions of 0.5, 0.25, and 0.125 cm^{-1}. Some samples were annealed to ∼32 K and recooled to 16 K, and additional spectra were obtained.

Computations were carried out using the Gaussian 98 package to confirm complex assignments.[22] The BPW91 and B3LYP density functional methods were used for all calculations,[23,24] and the electronic density of all atoms was represented by a 6-31+G(d,p) all electron basis set.[25] Geometries were fully relaxed during optimization, and initial starting orientations were given such that the CH···N angle was nearly collinear. The interaction energy was computed as $\Delta E_{int} = E_{complex} - (E_{Pccp} + E_{base})$, and the percent shift in the symmetric C−H stretch of Pccp upon complexation was formulated as $100(\nu_{complex} - \nu_{Pccp})/\nu_{Pccp}$. Vibrational frequencies were calculated analytically from second derivatives of the potential surface, and all energy values reported include zero-point energy corrections.

Results

Prior to any codeposition studies, blank experiments were carried out on each of the bases employed here. The resulting spectra were in excellent agreement with literature spectra[26−34] as well as with spectra recorded previously in this laboratory. Our blank Pccp experiments were in agreement with the only vibrational study published to date.[35] In addition, to ensure a precise comparison between parent and complex spectra, blank experiments were performed with each base such that argon (but no Pccp in plug) was deposited from one vacuum line and the base/argon sample from the other line so that the experiment was exactly duplicated but with no Pccp. In all experiments, we found that base/argon ratio of 1/250 with Pccp unrestricted yielded best results. In general, the spectral features observed when Pccp was codeposited with CH_3CN, NH_3, $(CH_3)NH_2$, and $(CH_3)_2NH$ are quite similar. Therefore, we discuss the first system in detail and the others in a somewhat comparative way.

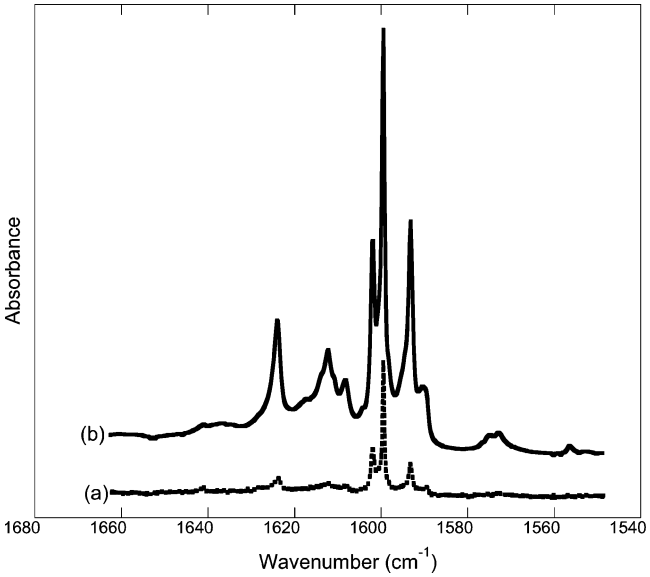

Figure 1. Infrared spectra (0.250 cm^{-1} resolution) in the N- - -H- - -Cl stretching region for parent $(CH_3)_3N$/Ar (trace a) and codeposition mixture Pccp/$(CH_3)_3N$/Ar (trace b) deposited on CsI at 16 K. There are no Pccp absorptions in this region.

Representative spectra are shown in Figures 1−6. Results not shown as spectra are listed in Tables 2 and 3.

Pccp + CH_3CN. The codeposition of samples of Ar/Pccp with Ar/CH_3CN gave rise to many new infrared absorptions that were not present in the spectra of the individual parents. Most notably, a band of medium intensity appeared at 3022.6 cm^{-1}, as a distinct shoulder to the red of the parent CH stretch at 3044.5 cm^{-1} which was also slightly shifted and its intensity increased greatly (Figure 2). This new band grew upon annealing. In addition, the broad, parent antisymmetric ring deformation at 954.6 cm^{-1} appeared as a doublet, with two narrow bands at 953.7 and 955.6 cm^{-1}. The most intense band at 955.6 cm^{-1} disappeared on annealing (Figure 5). The symmetric ring deformation appeared at 929.4 cm^{-1}, shifted slightly and greatly increased in intensity from the parent band at 927.4 cm^{-1}. In the region of the CCl stretch, a distinct new band appeared at 895.3 cm^{-1}, to the red of the parent band, which appears as a doublet (due to the presence of the two naturally occurring Cl isotopes) at 897.0 cm^{-1} (mean value of the doublet). There were additional slightly shifted, intense bands which fell within the envelope of the parent absorption, thus making the region complex. In the CCl_2 region of the spectrum, many new absorptions were noted. In the CCl_2 antisymmetric stretch (in-phase) region, three intense bands appeared at 772.4, 771, 3, and 769.1 cm^{-1}, to the red of the intense parent band at 773.0 cm^{-1}. In addition, two intense bands appeared to the blue of the parent band at 774.0 and 775.1 cm^{-1}. The band at 775.1 disappeared on annealing. In the region of the CCl_2 symmetric stretch (out-of-phase), two new bands appeared: one at 616.5 cm^{-1}, slightly red-shifted from the low-energy band of the parent doublet (616.0 cm^{-1}), and one at 618.1 cm^{-1}, to the blue of the high-energy parent doublet band at 617.6 cm^{-1}. This blue-shifted product band disappeared on annealing (Figure 3). In the region of the CCl_2 symmetric stretch (in-phase) a new band appeared at 532.2 cm^{-1}, shifted slightly from the parent band at 531.3 cm^{-1}. Three other new bands were noted at 526.7, 525.5, and 523.3 cm^{-1}, all of which fell within the envelope of a very weak, broad parent band centered at 524.0 cm^{-1}. The highest energy product band at 526.7 cm^{-1} disappeared on annealing. In addition to the new bands noted here, we observed significant increases in intensity for several modes, including the two CH

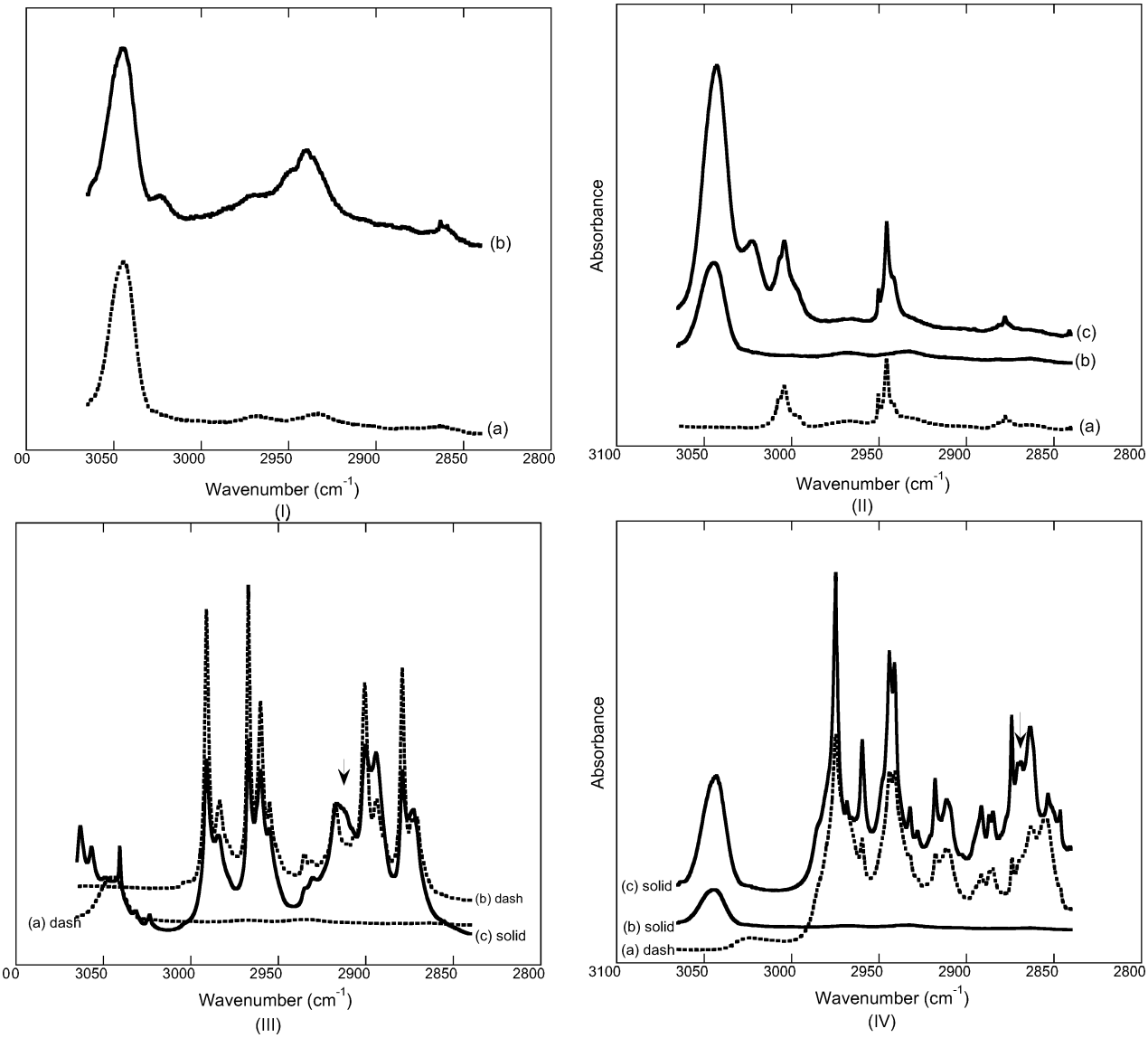

Figure 2. Infrared spectra (0.250 cm^{-1} resolution) in the CH stretching region for samples deposited on CsI at 16 K. Panel (I) shows Pccp/Ar (trace a) and codeposition mixture Pccp/NH_3/Ar (trace b). There are no NH_3 absorptions in this region. Panel (II) shows CH_3CN/Ar (trace a), Pccp/Ar (trace b), and Pccp/CH_3CN/Ar (trace c). Panel (III) shows Pccp/Ar (trace a), CH_3NH_2/Ar (trace b), and Pccp/CH_3NH_2/Ar. New product band is marked with an arrow. Panel (IV) shows Pccp/Ar (trace b), $(CH_3)_2NH$/Ar (trace a), and Pccp/$(CH_3)_2NH$/Ar. New product band is marked with an arrow.

TABLE 1: Experimental and DFT Results for the Hydrogen Stretching Mode, ν_s, and Other Hydrogen Bond Parameters for Pentachlorocyclopropane−Base Complexes

	Pccp	CH_3CN		NH_3		$(CH_3)NH_2$		$(CH_3)_2NH$	
	ν_s	ν_s	$\Delta\nu_s$	ν_s	$\Delta\nu_s$	ν_s	$\Delta\nu_s$	ν_s	$\Delta\nu$
observed (cm^{-1})	3044.5	3022.6	−21.9	2940.2	−104.3	2916.4	−128.1	2874.2	−170.3
calculated (B3LYP)	3192.8	3172.6	−20.2	3047.4	−145.4	3013.8	−179.0	2993.9	−198.9
calculated (BPW91)	3127.6	3091.5	−36.1	2914.5	−213.1	2872.1	−255.5	2833.9	−293.7
binding energy of Pccp−base (kcal/mol)									
B3LYP		3.0		4.0		4.1		4.2	
BPW91		1.9		3.3		3.3		3.5	
C−H- - -N bond distance (Å)									
B3LYP		2.310		2.173		2.146		2.140	
BPW91		2.360		2.120		2.112		2.097	

bending modes at 1295.6 cm^{-1} (mean value of doublet) and 1086.6 cm^{-1} (mean value of doublet, Figure 6) and a ring deformation mode at 1204.5 cm^{-1}. We also observed significant increases in intensity and new bands between 912.0 and 903.0 cm^{-1}, in the region of a combination band ($\upsilon_7 + \upsilon_8$, the addition of an in-phase CCl_2 wag with the in-phase CCl_2 symmetric stretch). Finally, we observed no changes in base modes with the exception of an increase in intensity of the CN stretching mode.

Pccp + NH_3. When Ar/Pccp was codeposited with Ar/NH_3, many new absorptions were observed that were not present in the spectra of the parents. One of the most prominent spectral

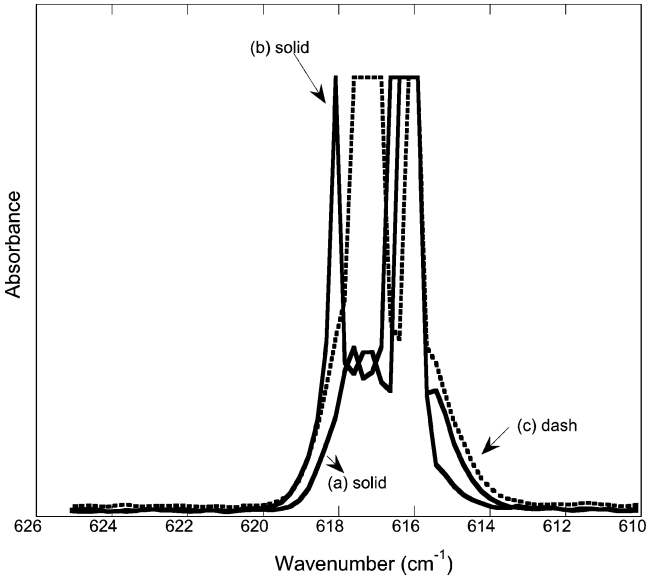

Figure 3. Infrared spectra (0.250 cm^{-1} resolution) in the region of the out-of-phase, symmetric CCl_2 stretch for Pccp/Ar (trace a), Pccp/CH_3CN/Ar (trace b), and annealed Pccp/CH_3CN/Ar (trace c). There are no CH_3CN absorptions in this region.

features observed was a new product band at 2940.2 cm^{-1}, which appeared to the red of the parent CH stretch at 3044.5 cm^{-1} (Figure 2). In the region of the CCl_2 symmetric stretch, the sharp and intense parent band at 531.3 cm^{-1} disappeared (became very weak and broad) and the broad, weak parent band at 524.0 cm^{-1} doubled in intensity. Upon annealing, a new very intense band appeared at 521.3 cm^{-1} (Figure 4). Finally, we observed a new, intense product band at 1018.0 cm^{-1}, blue-shifted from an NH_3 parent band (which appeared as a doublet, mean value reported) at 974.3 cm^{-1}.

Pccp + $(CH_3)NH_2$. When Ar/Pccp was codeposited with Ar/$(CH_3)NH_2$, many new absorptions were noted. A new band appeared at 2916.4 cm^{-1}, to the red of the parent CH stretch at 3044.5 cm^{-1}. This band appeared amidst the CH_3 stretching region of the base, but careful study including control experiments (all conditions identical but no Pccp in the manifold) supports this band as being a new product band (Figure 2). In addition, a new band appeared as a shoulder on the high-energy side of the parent CH bend (out of plane, 1090.0 cm^{-1}, Figure 6). In the region in between the parent CH bending mode and the parent ring breathing mode, we observed new bands at 1230.0 and 1247.3 cm^{-1} as well as a new shoulder on the high-energy side of the parent ring mode at 1204.5 cm^{-1}. In addition to the many new bands associated with Pccp modes, we noted intensity increases in some CH_3 modes and in the CN stretch of the base.

Pccp + $(CH_3)_2NH$. When Ar/Pccp was codeposited with Ar/$(CH_3)_2NH$, a new band was observed at 2874.2 cm^{-1}, to the red of the parent CH stretch at 3044.5 cm^{-1}. Again, this new product band fell in a region of base modes, but its growth was apparent (Figure 2). We also observed a distinct new product band at 1247 cm^{-1}, in between a parent CH bending mode and a ring breathing mode. In addition, both the CH bending mode and ring breathing modes showed a dramatic increase in intensity. In the region of the antisymmetric ring deformation, we observed a huge increase in intensity of the parent band at 954.6 cm^{-1}. Upon annealing, this band decreased in intensity, and a new, intense band was noted at 952.0 cm^{-1} (Figure 5). In the region of the CCl_2 symmetric ring deformation, two new very intense and distinct product bands appeared (932.8, 928.0 cm^{-1}). On annealing, both of these bands disappeared and a new band appeared at 926.0 cm^{-1}. Finally, we observed

TABLE 2: Observed and Calculated Vibrational Frequencies (cm^{-1}) and Intensities (km/mol) Associated with the Pentachlorocyclopropane−Acetonitrile Complex

	Pccp			Pccp−CH_3CN		
mode[a]/symmetry	obsd	calcd	int	obsd/shift	calcd/shift	int
			B3LYP/6-31+G(d,p)			
ν_1 CH stretch/a′	3044.5	3192.8	(6)	3022.6/−21.9	3172.6/−20.2	(182)
ν_2 CH bend/a′	1295.6[b]	1323.9	(4)	1295.6[b,c]	1343.1/+19.2	(7)
ν_3 ring/a′	1204.5	1232.6	(5)	1204.5[c]	1243.8/+11.2	(2)
ν_{13} CH bend/a″	1086.6[b]	1108.6	(3)	1086.6[b,c]	1149.8/+41.2	(2)
ν_{14} ring/a″	954.6	971.4	(21)	953.7[d]/−0.9	968.2/−3.2	(18)
ν_4 ring/a′	927.4	928.6	(18)	929.4/+2.0	932.3/+3.7	(8)
ν_5 CCl stretch/a′	897.0[b]	887.1	(117)	895.3[d]/−1.7	883.2/−3.9	(105)
ν_{15} CCl_2 stretch/a″		862.3	(2)		867.3/+5.0	(3)
ν_6 CCl_2 stretch/a′	773.0	750.6	(96)	769.1[e]/−3.4	747.1/−3.5	(109)
ν_{16} CCl_2 stretch/a″	617.0[b]	620.2	(22)	616.5[d]/−0.5	619.1/−1.1	(21)
ν_7 CCl_2 stretch/a′	531.3	536.8	(13)	532.2/+0.9	538.4/+1.6	(14)
ν_{19} CCl bend	524.0	523.2	(11)	523.3[e]/−0.7	521.6/−1.6	(21)
			BPW91/6-31+G(d,p)			
ν_1 CH stretch/a′	3044.5	3127.6	(5)	3022.6/−21.9	3091.5/−36.1	(176)
ν_2 CH bend/a′	1295.6[b]	1274.0	(4)	1295.6[b,c]	1292.0/+18.0	(7)
ν_3 ring/a′	1204.5	1189.2	(4)	1204.5[c]	1199.1/+9.9	(1)
ν_{13} CH bend/a″	1086.6[b]	1063.6	(3)	1086.6[b,c]	1103.6/+40.0	(2)
ν_{14} ring/a″	954.6	930.2	(30)	953.7[d]/−0.9	927.9/−2.3	(28)
ν_4 ring/a′	927.4	889.9	(28)	929.4/+2.0	891.6/+1.7	(25)
ν_5 CCl stretch/a′	897.0[b]	855.5	(130)	895.3[d]/−1.7	853.8/−1.7	(119)
ν_{15} CCl_2 stretch/a″		826.7	(3)		833.9/+7.2	(5)
ν_6 CCl_2 stretch/a′	773.0	729.8	(107)	769.1[e]/−3.4	727.1/−2.7	(119)
ν_{16} CCl_2 stretch/a″	617.0[b]	602.2	(24)	616.5[d]/−0.5	601.3/−0.9	(24)
ν_7 CCl_2 stretch/a′	531.3	524.2	(12)	532.2/+0.9	525.8/+1.6	(14)
ν_{19} CCl bend	524.0	511.3	(10)	523.3[e]/−0.7	508.8/−2.5	(22)

[a] Vibrational modes: ν_3 = ring breathing; ν_{14} = antisymmetric ring deformation; ν_4 = symmetric ring deformation; ν_5 CCl stretch = symmetric; ν_{15} CCl_2 stretch = antisymmetric, out-of-phase; ν_6 CCl_2 stretch = antisymmetric, in-phase; ν_{16} CCl_2 stretch = symmetric, out-of-phase; ν_7 CCl_2 stretch = symmetric, in-phase. From ref 35. [b] Doublet, mean value reported. [c] No shift, but increase in intensity. [d] Red-shifted product reported. Blue-shifted product disappears upon annealing. [e] Several new product bands, but largest red-shifted product reported.

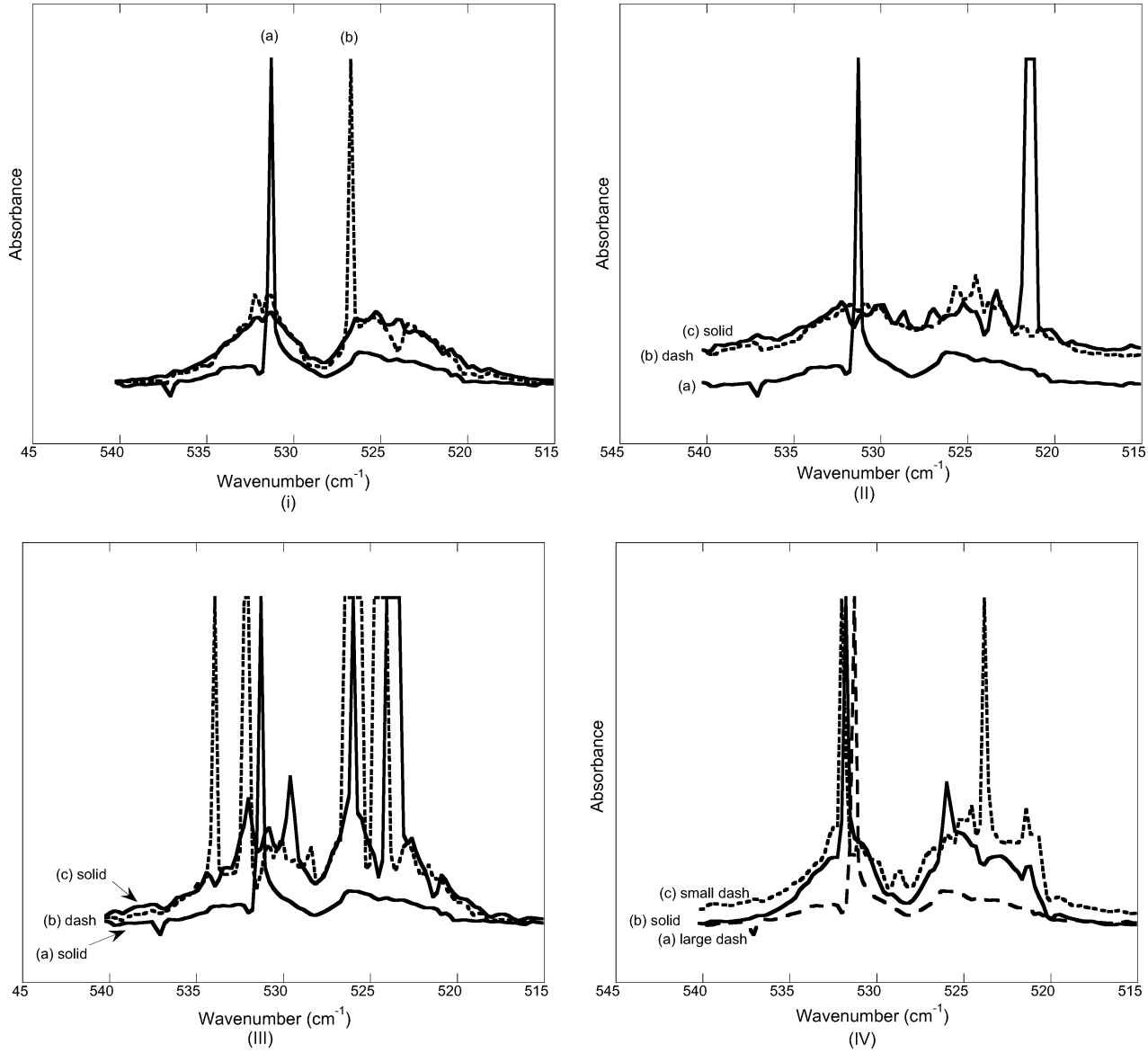

Figure 4. Infrared spectra (0.250 cm^{-1} resolution) in the region of two fundamentals—a symmetric CCl_2 stretch and a CCl bend—for samples deposited on CsI at 16 K. Panel (I) shows Pccp/Ar (trace a), Pccp/CH_3CN/Ar (trace b), and annealed Pccp/CH_3CN/Ar (unlabeled solid trace). Panel (II) shows Pccp/Ar (trace a), Pccp/NH_3/Ar (trace b), and annealed Pccp/NH_3/Ar (upper solid trace c). Panel (III) shows Pccp/Ar (trace a), Pccp/$(CH_3)NH_2$/Ar (trace b), and annealed Pccp/$(CH_3)NH_2$/Ar (trace c). Panel (IV) shows Pccp/Ar (trace a), Pccp/$(CH_3)_2NH$/Ar (trace b), and annealed Pccp/$(CH_3)_2NH$/Ar (trace c). There are no base absorptions in this region.

increases in the intensity of many base modes, the most significant at 2832.0, 2792.8, and 1021.0 cm^{-1}.

Pccp + $(CH_3)_3N$. When Ar/Pccp was codeposited with Ar/$(CH_3)_3N$, three distinct new absorptions were noted at 1623.8. 1612.0, and 1608.0 cm^{-1}. Also, a weak, broad doublet was observed with maxima at 1573.0 and 1575.0 cm^{-1} (Figure 1). In addition, the CH stretch of the Pccp disappeared, as did the ring modes.

Computational Results

Chemical properties indicating the strength of a hydrogen bond include bond energy, bond lengths and angles, and relative vibrational shift of a symmetric carbon−hydrogen stretching mode. Both theoretical methods predicted the acetonitrile−Pccp complex to have the smallest ΔE_{int} (2.9 and 1.9 kcal/mol at the B3LYP and BPW91 levels, respectively). Ammonia, monomethylamine, and dimethylamine−Pccp complexes were all calculated to have binding energies in the range 4.0−4.2 and 3.3−3.5 kcal/mol at these two theoretical levels, respectively (Table 1). The addition of methyl groups to ammonia shortens the N−H and N−C distances (Figure 7). Our B3LYP calculations predicted a decrease in the N- - -H length from 2.173 to 2.140 Å for the ammonia−Pccp and dimethylamine−Pccp complexes and from 2.120 to 2.097 Å at the BPW91 level. These are roughly 12% larger than the distance predicted for the acetonitrile−Pccp complex. Also, the N−H−C angle is predicted to approach closest to linearity in the dimethylamine−Pccp complex, which is 1.4° (B3LYP) and 1.7° (BPW91) larger (i.e., closer to 180°) than the ammonia−Pccp complex. The shift in the hydrogen-bonded C−H stretching mode is predicted to become larger with the replacement of the H atoms on ammonia with methyl groups. Our B3LYP calculations predict this increase from 4.6% to 5.6% and 6.2% for the ammonia−Pccp, monomethylamine−Pccp, and dimethylamine−Pccp complexes, respectively. BPW91 predicts larger relative shifts in the same order ranging from 6.8% to 9.4% for these three complexes, which is considerably larger than that predicted for the acetonitrile−Pccp complex (1.2%). All of these computed structural

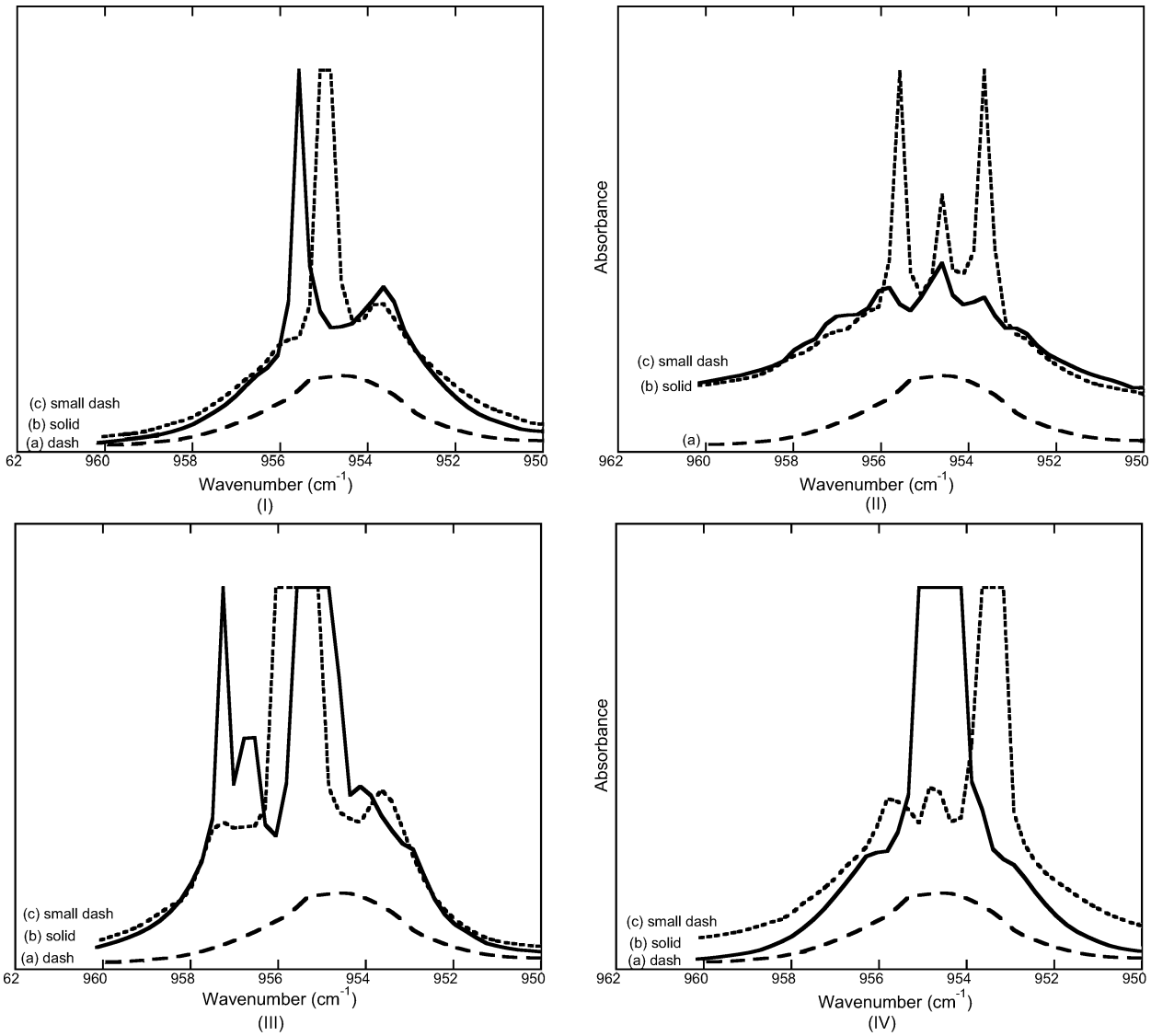

Figure 5. Infrared spectra (0.250 cm^{-1} resolution) in the region of the antisymmetric ring deformation for samples deposited on CsI at 16 K. Panel (I) shows Pccp/Ar (trace a), Pccp/CH_3CN/Ar (trace b), and annealed Pccp/CH_3CN/Ar (trace c). Panel (II) shows Pccp/Ar (trace a), Pccp/NH_3/Ar (trace c), and annealed Pccp/NH_3/Ar (trace b). Panel (III) shows Pccp/Ar (trace a), Pccp/$(CH_3)NH_2$/Ar (trace b), and annealed Pccp/$(CH_3)NH_2$/Ar (trace c). Panel (IV) shows Pccp/Ar (trace a), Pccp/$(CH_3)_2NH$/Ar (trace b), and annealed Pccp/$(CH_3)_2NH$/Ar (trace c). There are no base absorptions in this region.

parameters indicate that the ability of these four precursor molecules to form a substantial hydrogen bond with Pccp increases in the order acetonitrile < ammonia < monomethylamine < dimethylamine (Table 1).

Discussion

Evidence for interaction between Pccp and the bases comes from a direct comparison of the infrared spectra of the isolated hydrocarbon acid and bases (i.e., the blank or parent spectra) with those spectra obtained in the codeposition experiments. In the codeposition experiments with CH_3CN, NH_3, $(CH_3)NH_2$, and $(CH_3)_2NH$, new absorptions were observed close to but distinct from parent vibrational modes. In addition, some modes did not change at all while others changed in intensity but not frequency. These spectral changes are consistent with those that are known to occur as a result of hydrogen bond formation.[36−40] In the codeposition experiments with $(CH_3)_3N$, however, all Pccp modes completely disappeared while base modes remained relatively unchanged (but only a small amount of parent base remained). We also observed new and distinct bands. These observations argue in favor of a distinct chemical reaction (e.g., addition, elimination, or rearrangement of the subunits) in which bonds are broken and new bonds formed. From this we conclude that Pccp loses HCl to form tetrachlorocyclopropene and a trimethylamine:HCl complex. The bands we observe (Figure 1) correlate well with the N- - -H- - -Cl antisymmetric stretching region in the spectrum of the 1:1 trimethylamine:HCl complex.[41] For example, Ault and Pimentel report bands at 1615 and 1575 cm^{-1} in a nitrogen matrix, while we observe new bands at 1612.0 and 1608.0 cm^{-1} as well as a weak doublet with maxima at 1573.0 and 1575.0 cm^{-1}. We note that our bands are higher in energy than what is reported for an argon matrix but similar to the results in a nitrogen matrix. It is known that an increase in polarizability of the matrix host increases proton transfer from the HCl to the amine, resulting in higher energy product bands.[21b] Although we are working with an Ar matrix host, it is possible that the presence of Pccp and other chlorinated products increases the polarizability of our matrix. Since we do not observe a tetrachlorocyclopropene spectrum, we conclude that there is some further ring-opening reaction occurring in

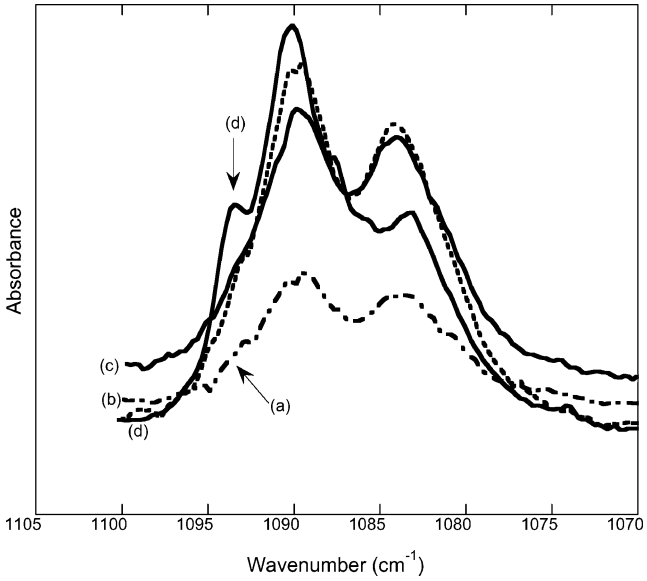

Figure 6. Infrared spectra (0.250 cm^{-1} resolution) in the CH out-of-plane bending region for Pccp/Ar (trace a), Pccp/$(CH_3)_2NH$/Ar (trace b), Pccp/CH_3CN/Ar (trace c), and Pccp/$(CH_3)NH_2$/Ar (trace d). New product absorption is marked with an arrow. Pccp/NH_3/Ar is omitted for clarity as it overlaps with trace c. There are no base absorptions in this region.

the matrix. Further work on this system is ongoing in our laboratory.

Several experimental observations support that the complexes formed between Pccp and the bases CH_3CN, NH_3, $(CH_3)NH_2$, and $(CH_3)_2NH$ are in fact hydrogen-bonded complexes with 1:1 stoichiometry. The most compelling evidence for this is the fact that product bands were observed over a wide range of reagent concentrations and matrix conditions. In addition, Pccp, with five halogens and only one proton, has one site for hydrogen bond formation. Numerous studies of halogenated alkanes, alkenes, and alkynes demonstrate that there is no propensity for protons on the base to interact with the halogen substituents on the hydrocarbon.[38,39] Thus, we can be certain that Pccp hydrogen-bonds to the N of the base, forming a C−H- - -N linkage. We note that it is possible for two kinds of nitrile compounds to form, a complex to the lone pair of the nitrogen or to the π electrons of the CN triple bond.[42−46] If coordination to the triple bond occurs, then a large decrease in the CN stretching vibration frequency is expected.[47] On the other hand, coordination to the N results in a characteristic increase in the CN stretching frequency.[48] The latter is precisely what we observe, and DFT calculates a 5 cm^{-1} blue shift and a significant increase in intensity for this mode. In fact, our DFT results support the formation of a C−H- - -N hydrogen bond for Pccp with the bases CH_3CN, NH_3, $(CH_3)NH_2$, and $(CH_3)_2NH$ (Figure 7).

The observable most commonly used in the characterization of hydrogen-bonded systems is the shift of the parent C−H stretch that involves the hydrogen-bonded hydrogen. Numerous studies involving alkynes[36−38] and alkenes[39,40] confirm that this shift, usually referred to as $\Delta\nu_s$, is a reliable measure of the strength of interaction. In our previous study of bromocyclopropane−base complexes,[12] we did not observe a distinct C−H stretch, as that region of the spectrum was congested with several weak and broad overlapping bands, together which were about 110 cm^{-1} wide. It is likely that the shift in this mode (which was calculated to be about 7 cm^{-1}) fell beneath these parent absorptions. In the case of Pccp, however, the C−H stretching region was relatively straightforward to study and provides the most compelling evidence for hydrogen bond formation (Figure

TABLE 3: Observed and Calculated Vibrational Frequencies (cm^{-1}) and Intensities (km/mol) Associated with the Pentachlorocyclopropane−Amine Complexes

	Pccp			Pccp−NH_3			Pccp−$(CH_3)NH_2$			Pccp−$(CH_3)_2NH$		
mode	obsd	calcd	int	obsd/shift	calcd/shift	int	obsd/shift	calcd/shift	int	obsd/shift	calcd/shift	int
						B3LYP/6-31+G(d,p)						
ν_1	3044.5	3193.0	(6)	2940.2/−104.3	3047.4/−145.4	(363)	2916.4/−128.1	3013.8/−179.0	(234)	2874.2/−170.3	2993.9/−198.9	(276)
ν_2	1295.6[b]	1324.0	(4)	1295.6[b,c]	1378.6/+54.7	(7)	1295.6[b,c]	1382.9/+59.0	(9)	1295.6[b,c]	1386.5/+62.6	(10)
ν_3	1204.5	1232.6	(5)	1205.2/+0.7	1253.2/+20.6	(3)	1205.4/+0.9	1253.8/+21.2	(4)	1203.5/−1.0	1253.0/+20.4	(5)
ν_{13}	1086.6[b]	1108.6	(3)	1086.6[b,c]	1196.1/+87.5	(3)	1092.0[g]/+5.4	1205.9/+97.3	(2)	1092.0[g]/+5.4	1209.9/+101.3	(3)
ν_{14}	954.6	971.4	(21)	953.6/−1.0	969.1/−2.3	(20)	955.0/−0.4[d]	969.8/−1.6	(20)	954.6[c]	969.7/−1.7	(19)
ν_4	927.4	928.6	(18)	927.4[c]	932.8/+4.2	(20)	931.0/+3.6[h]	933.3/+4.7	(21)	934.0[h]/+6.6	933.4/+4.8	(225)
ν_5	897.0[b]	887.1	(117)	895.8/−1.2	880.6/−6.5	(101)	895.3/−1.7	879.7/−7.4	(119)	893.3[e]/-3.7	879.4/−7.7	(98)
ν_{15}	(−)	862.3	(2)	(−)	869.8/+7.5	(4)	(−)	869.4/+7.1	(20)	(−)	870.3/+8.0	(5)
ν_6	773.0	750.6	(96)	769.0[b]/-4.0	744.5/−7.1	(114)	766.7/−6.3[e]	743.5/−7.1	(115)	765.5[e]/-7.5	742.5/−8.1	(119)
ν_{16}	617.0[b]	620.2	(22)	615.0/−2.0	618.7/−1.5	(21)	615.5/−1.5[d]	618.6/−1.6	(21)	615.5[d]/-1.5	618.6/−1.6	(20)
ν_7	531.3	536.8	(13)	(−)[f]	545.3/+8.5	(19)	533.0/+1.7	545.2/+8.4	(14)	533.0/+1.7	545.8/+9.0	(13)
ν_{19}	524.0	523.2	(11)	523.0/−1.0[e]	522.6/−0.6	(22)	523.0/−1.0[e]	522.2/−1.0	(26)	521.4[e]/-2.6	521.5/−1.7	(27)
						BPW91/6-31+G(d,p)						
ν_1	3044.5	3127.6	(5)	2940.2/−104.3	2914.5/−213.1	(519)	2916.4/−128.1	2872.1/−255.5	(711)	2874.2/−170.3	2833.9/−293.7	(951)
ν_2	1295.6[b]	1274.0	(4)	1295.6[b,c]	1337.4/+63.4	(7)	1295.6[b,c]	1342.1/+68.1	(11)	1295.6[b,c]	1346.7/+72.7	(11)
ν_3	1204.5	1189.2	(4)	1205.2/+0.7	1209.9/+20.7	(6)	1205.4/+0.9	1209.9/+20.7	(9)	1203.5/−1.0	1208.4/+19.2	(16)
ν_{13}	1086.6[b]	1063.6	(3)	1086.6[b,c]	1163.9/+100.3	(3)	1092.0/+5.4	1171.4/+107.8	(2)	1092.0[d]/+5.4	1177.8/+114.2	(3)
ν_{14}	954.6	930.2	(30)	953.6/−1.0	931.8/+1.6	(28)	955.0/−0.4[d]	931.3/+1.1	(28)	954.6[c]	930.9/+0.7	(28)
ν_4	927.4	889.9	(28)	927.4[c]	892.9/+3.0	(26)	931.0/+3.6[h]	895.1/+5.2	(38)	934.0[h]/+6.6	896.8/+6.9	(33)
ν_5	897.0[b]	855.5	(130)	895.8/−1.2	848.9/−6.6	(110)	895.3/−1.7	846.8/−8.7	(114)	893.3[e]/-3.7	845.5/−10.0	(96)
ν_{15}	(−)	826.7	(3)	(−)	835.0/+8.3	(6)	(−)	833.8/+7.1	(10)	(−)	833.0/+6.3	(7)
ν_6	773.0	729.8	(107)	769.0[b]/-4.0	723.5/−6.3	(127)	766.7/−6.3[e]	721.2/−8.6	(130)	765.5[e]/-7.5	720.1/−9.7	(137)
ν_{16}	617.0[b]	602.2	(24)	615.0/−2.0	600.4/−1.8	(24)	615.5/−1.5[d]	600.4/−1.8	(23)	615.5[d]/-1.5	600.2/−2.0	(23)
ν_7	531.3	524.2	(12)	(−)[f]	535.6/+11.4	(19)	533.0/+1.7	534.8/+10.6	(15)	533.0/+1.7	535.0/+10.8	(13)
ν_{19}	524.0	511.3	(10)	523.0/−1.0	510.8/−0.5	(25)	523.0/−1.0[e]	509.3/−2.0	(30)	521.4[e]/-2.6	508.3/−3.0	(34)

[a] Vibrational modes: ν_3 = ring breating; ν_{14} = antisymmetric ring deformation; ν_4 = symmetric ring deformation; ν_5 CC1 stretch = symmetric; $\nu_{15}CC1_2$ stretch = antisymmetric, out-of-phase; ν_6 $CC1_2$ stretch = antisymmetric, in-phase; $\nu_{16}CC1_2$ stretch = symmetric, out-of-phase; ν_7 $CC1_2$ stretch = symmetric, in-phase. From ref 35. [b] Doublet, mean value reported. [c] No shift, but increase in intensity. [d] Red-shifted product reported. Blue-shifted product disappears upon annealing. [e] Several new product bands, but largest red-shifted product reported. [f] Band disappears in codeposition. [g] Shoulder. [h] Many new bands/complex region. Most prominent band reported.

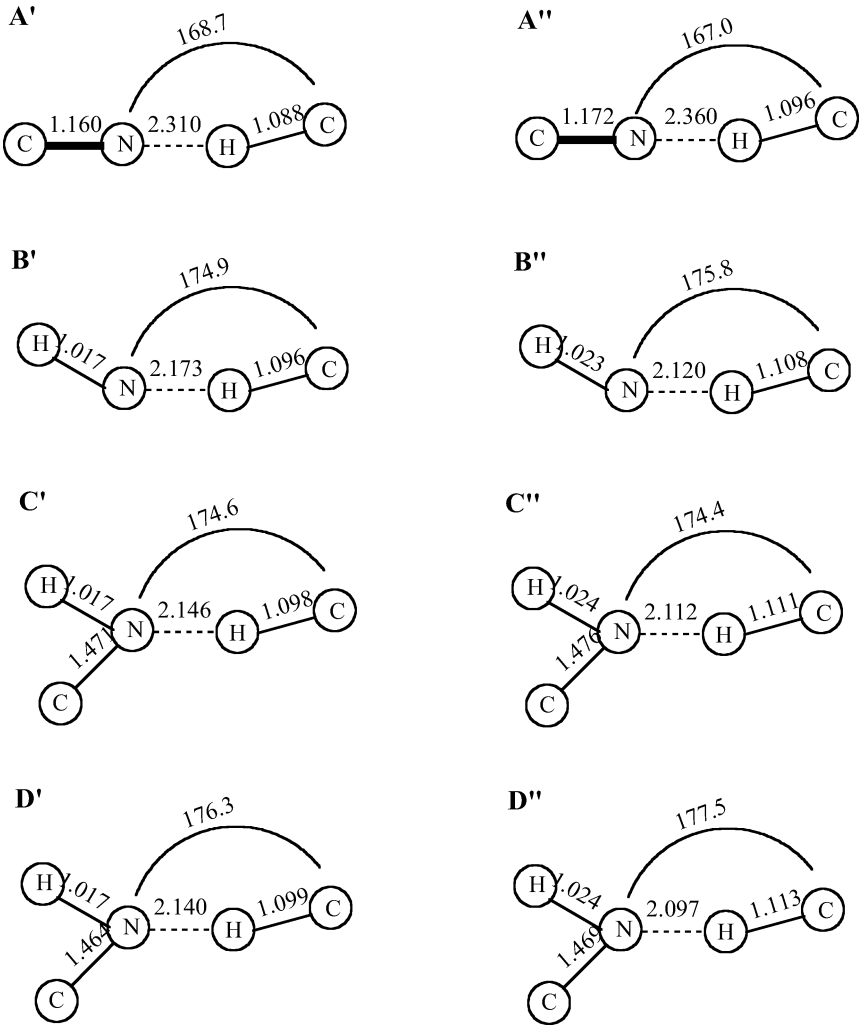

Figure 7. Important geometrical values of the (A) acetonitrile−Pccp, (B) ammonia−Pccp, (C) monomethylamine−Pccp, and (D) dimethylamine−Pccp complexes computed with the (′) B3LYP and (″) BPW91 density functionals. All bond lengths are in angstroms and angles are in degrees.

2). We note that the C−H stretch for Pccp is well-known, and at the time the vibrational spectrum of Pccp was recorded, it was hoped that it would provide an unequivocal location for the C−H stretching mode in monosubstituted cyclopropanes since Pccp has no interfering methylene groups. The shifts reported here (Table 1), which range from 22 to 170 cm^{-1}, are smaller than for many traditional hydrogen bonds, but similar to other systems with hydrogen bonds involving a CH group. Previous studies show that the hydrogen-bonding interaction between a series of alkynes with a range of bases was characterized by a red shift of 20−300 cm^{-1} for the alkynic hydrogen stretching motion,[36−38] and complexes of ethylene and substituted ethylenes with a range of bases yielded shifts which ranged from 10 to 150 cm^{-1}.[39,40] Thus, the range observed for Pccp with bases is similar to that of alkenes, supporting the theory that cyclopropanes behave more like olefins than alkanes because of the high degree of ring strain. It is interesting to note that the calculated shift for BrCp-NH_3 (∼7 cm^{-1}) is much less than the calculated shift of 145 cm^{-1} (B3LYP) for Pccp−NH_3, suggesting that the five Cl substituents play a major role in increasing the strength of the hydrogen-bonding interaction. This is not surprising since we reported in our BrCp study that *only one* Br substituent was necessary to activate the C−H group to form a C−H- - -N hydrogen bond (there was no evidence of complex formation with Cp and bases).[12] In addition, previous matrix work demonstrates that the greater number of halogens on the substituted hydrocarbon, the greater the shift, because the electron-withdrawing nature of the halogens increases the acidity of the acidic proton.[38,39] The calculated binding energy of the complexes correlates well with our observed shifts (see Table 1). As can be seen, our most weakly hydrogen-bonded complex has a binding energy greater than that of BrCp−NH_3 (2.35 kcal/mol, MP2), and the Pccp−NH_3 complex has a binding energy that is 1.60 kcal/mol greater than that of BrCp−NH_3. This makes sense, and in fact Radom et al. studied the effects of electronegative substitution on the strength of C−H- - -N hydrogen bonds and found that there is a monotonic progression toward stronger bonds with successive substitution in all cases. He also found that the effect of electronegative substituents on the binding energy of the complex increases with respect to hybridization of the proton donor in the order $sp < sp^2 < sp^3$.[49] Since for cyclopropane the hybridization of the C is approximately $sp^{2.28}$,[17,18] pentasubstitution should be quite significant.

In this study, the general ordering of $\Delta\nu_s$ with the bases that formed a C−H- - -N hydrogen bond with Pccp was $(CH_3)_2NH$ > $(CH_3)NH_2$ > NH_3 > CH_3CN. This trend makes sense since, in general, the gas-phase basicities of alkylamines increase with successive methyl substitution due to the inductive effect of methyl groups.[50] Our current work also demonstrates that trimethylamine is a strong enough base to remove HCl from Pccp, thus forming a trimethylamine:HCl complex rather than a C−H- - -N hydrogen bond. The DFT results at the B3LYP level agree well with our experimental observations for $\Delta\nu_s$,

and in general they correlate more closely with experiment than do the BPW91 results (Tables 1 and 3). Although there are claims in the literature that the MP2/6-31+G(d,p) level of theory is the minimum level required to obtain reliable geometries of hydrogen-bonded complexes,[51] there are numerous studies that report that the B3LYP/6-31+G(d,p) level of theory results agree extremely well with experimental shift values and provide accurate and reliable structural information for hydrogen-bonded complexes.[52]

Additional modes of the Pccp were perturbed by hydrogen bond formation. This is characteristic of hydrogen bond formation, where the proton donor and proton acceptor subunits in the newly formed linkage are perturbed by the new interaction. In particular, if a vibrational mode causes the region of the molecule associated with the hydrogen bond to be displaced, then it is likely to see a shift in that mode. In the case of Pccp, CCl and CCl_2 modes as well as several ring modes changed significantly. We also observed changes in a combination band involving a symmetric CCl_2 stretch and a CCl_2 wag. Although we discuss these modes below, we note that these regions of the spectrum were quite complex. In the case of CCl and CCl_2 modes, many new, very intense bands appeared both within the envelope of the parent absorption and also as shoulders. The splitting in these parent bands arises from the presence of both ^{37}Cl and ^{35}Cl in natural abundance as well as from matrix effects. Specifically, splitting can arise because of slightly different packing sites within the argon matrix or from the trapping of slightly different conformers of the complex (which is also an effect of the argon lattice packing).[53] In this study, it is difficult to tell which of these is causing the splitting. Nonetheless, there is valuable information to be obtained from examining these additional perturbed modes. We emphasize here that although the data in certain regions was complex, we did our best to tabulate it so it could be compared to theory. As can be seen from examining Tables 2 and 3, we were often able to report products as either mean values of a doublet or multiplet or to report a prominent band that agreed with the DFT prediction. In many cases the overall shift and magnitude of our product bands correlate well with predicted results.

For all of the complexes, we observed either distinct, very intense absorptions or shoulders on both the high- and low-energy sides of the parent CCl and CCl_2 stretching modes. In addition, there were many new, narrow, and intense bands within the envelope of the parent absorptions. Upon annealing, the product band on the high-energy side of the parent bands disappeared. From this we conclude that this blue-shifted product either is a conformer that changes upon annealing or simply represents a site that converts to another. It is worth noting that if we consider the product band on the low-energy side of the parent band as our stable product in cases where the blue-shifted product disappears on annealing, then our experiment agrees well with the DFT results (Tables 2 and 3). For example, for Pccp$-CH_3CN$, in the region of the symmetric CCl_2 stretch (out of phase), we observed a new band at 618.0 cm^{-1} and one at 615.0 cm^{-1}, shifted 2 cm^{-1} to the blue and 1 cm^{-1} to the red of the parent band, respectively. The band at 618.0 cm^{-1} disappears upon annealing (Figure 3), and thus the DFT prediction of a 1.1 cm^{-1} red shift for this mode supports our conclusions. In previous work involving alkenes with bases, similar results were obtained. Specifically, Ault et al. reported either a distinct absorption or a shoulder on the low-energy side of one of the C−X stretching modes, with shifts on the order of 3−10 cm^{-1}, demonstrating slight electron density rearrangement upon hydrogen bond formation.[40] Our shifts are on the order of 2−5 cm^{-1}. The range of shifts predicted by DFT theory is approximately 1−5 cm^{-1}, and in general, the direction of the shift agrees with our experiment.

A region of the spectrum worth noting is 540−520 cm^{-1}, which spans two Pccp fundamentals—a symmetric CCl_2 stretch (in-phase) at 531.4 cm^{-1} and a CCl bend (out of plane) at 524.0 cm^{-1} (Figure 4). The CCl bend is the only Pccp fundamental vibration not assigned in the original and only Pccp vibrational study done, as the authors state that they could not find it.[35] We observe a weak, broad absorption at 524.0 cm^{-1}, and DFT calculates a parent mode at 523.2 cm^{-1} which we are confident, based on displacement coordinates, is in fact the CCl bend. Prior to obtaining the DFT results, we, too, would have missed this fundamental. With each base, the CCl_2 symmetric stretch is predicted to blue shift and the CCl bend is predicted to red shift, and this is what we observe. We also note that in some cases there is a product band to the blue of the parent CCl bend which disappears upon annealing.

The specific ring modes perturbed on hydrogen bond formation were the ring breathing mode and both the symmetric and antisymmetric ring deformations. With all bases, both the ring breathing mode at 1204.5 cm^{-1} and the symmetric ring deformation mode at 927.4 cm^{-1} increased in intensity. In the region of the antisymmetric ring deformation mode we generally observed a blue-shifted product (again, which disappeared upon annealing) and a red-shifted product band about 1 cm^{-1} from the parent band (Figure 5). DFT predicts a small red shift in this mode for all of the bases.

Another characteristic spectral change upon hydrogen bond formation is a shift to higher energy of the proton donor bending modes. Previous work with alkenes[39,40] supports this as does work from this laboratory on complexes of bromocyclopropane with N bases.[12] Specifically, coordination of the proton adjacent to the Br substituent on the cyclopropane ring to the N of the base was evidenced by a shift of 12 cm^{-1} for the in-plane bend and 6 cm^{-1} for the out-of-plane bend. With Pccp, we observed no shift but an increase in intensity in the two CH bending modes, except in the case of Pccp$-(CH_3)NH_2$ where we observed a shoulder on the high-energy side of the parent out-of-plane bending mode (Figure 6). These results were quite unexpected, especially since the DFT predicts significant shifts in these modes (Tables 2 and 3). We are not sure why we do not observe a shift in these modes upon hydrogen bond formation. One possibility is that the product bands are too weak to be seen. DFT does in fact predict these modes to be of low intensity. Another possibility is that this results from a matrix effect that the DFT cannot account for. One striking observation we noted upon viewing the animated vibrations for Pccp (and looking at displacement coordinates) is that the C−H group swings quite far from side to side during these bending motions. Perhaps this range of motion is restricted in the argon lattice, and thus there is not as much of a change in the dipole moment derivative upon hydrogen bond formation as is calculated.

Finally, we note that many base modes were significantly increased upon hydrogen bond formation. The only base for which we observed a significant shift was NH_3. In the case of Pccp$-NH_3$, the symmetric deformation or "umbrella" mode of ammonia was blue-shifted by 45 cm^{-1}. This mode has been shown to be sensitive to complex formation in previous matrix studies.[37,38] DFT (B3LYP) predicted a shift of 93 cm^{-1} for this mode. In our previous BrCp-NH_3 study, we did not observe a shift in this mode.[12] That we observe such a large shift here is indicative of a stronger C−H- - -N hydrogen bond.

Conclusions

This work represents the first detailed matrix isolation study of Pccp both as a parent species and with the bases acetonitrile, ammonia, monomethylamine, dimethylamine, and trimethylamine. Both IR spectroscopy and DFT calculations support the formation of 1:1 complexes between Pccp and the bases acetonitrile, ammonia, monomethylamine, and dimethylamine. The most compelling evidence of complex formation comes from changes in the CH stretching mode, ν_s, which is the observable most commonly used in the characterization of hydrogen-bonded systems. In addition, changes in many other Pccp modes and in some base modes as well fully support the formation of these complexes. Although some regions of the spectra are complicated by isotope effects as well as matrix effects, there are new product bands which agree with the DFT predictions, especially at the B3LYP level of theory. This work provides an interesting comparison with bromocyclopropane, the molecular inverse of Pccp, and serves, in a comparative way, to elucidate the effect of substitution on the nature and strength of the important C−H- - -N hydrogen bond.

Acknowledgment. We gratefully acknowledge support of this research by the National Science Foundation through Grant CHE-0107777 (under the Research in Undergraduate Institutions program). We especially thank Dickinson College for supplying substantial funding for the rebuilding of Professor Samet's matrix-isolation laboratory following a flood. Special thanks to Lester Andrews and Jonathan Lyon for the computational support on this project.

References and Notes

(1) See, for example: (a) Pimentel, G. C.; McClellan, A. L. *The Hydrogen Bond*; W.H. Freeman: San Francisco, 1960. (b) Pauling, L. *The Nature of the Chemical Bond*; Cornell University Press: Ithaca, NY, 1960.

(2) Taylor, R.; Kennard, O. *J. Am. Chem. Soc.* **1982**, *104*, 5063.

(3) See, for example: Desiraju, G. R.; Steiner, T. *The Weak Hydrogen Bond in Structural Chemistry and Biology*; Oxford University Press: New York, 1999 and references therein.

(4) Smith, D. L. *Eng. Sci.* **1994** (Fall), 27.

(5) See for example: Scaccianoce, L.; Braga, D.; Calhorda, M. J.; Grepioni, F.; Johnson, B. F. G. *Organometallics* **2000**, *19*, 790 and references therein.

(6) See, for example: (a) Engdahl, A.; Nelander, B. *Chem. Phys. Lett.* **1983**, *100*, 129. (b) Peterson, K. I.; Klemperer, W. *J. Chem. Phys.* **1984**, *81*, 3842. There are many others. This is not meant to be a comprehensive review. Also see ref 3 above.

(7) Yohannan, S.; Faham, S.; Yang, D.; Grosfeld, D.; Chamberlain, A. K.; Bowie, J. U. *J. Am. Chem. Soc.* **2004**, *126*, 2284.

(8) See, for example: (a) Reddy, D. S.; Goud, B. S.; Panneerselvam, K.; Desiraju, G. R. *J. Chem. Soc., Chem. Commun.* **1993**, 663. (b) Sigel, R. K. O.; Freisinger, E.; Metzger, S.; Lippert, B. *J. Am. Chem. Soc.* **1998**, *120*, 12000. There are others. This is not meant to be a comprehensive review.

(9) Ikezaki, A.; Nakamura, M. *Inorg. Chem.* **2003**, *42*, 2301.

(10) See, for example: Radom, L.; Hartmann, M. *J. Phys. Chem. A* **2000**, *104*, 968 and references therein.

(11) Meyer, M.; Suhnel, J. *J. Biomol. Struct. Dyn.* **2001**, *18*, 545.

(12) Bedell, B. L.; Goldfarb, L.; Mysak, E. R.; Samet, C.; Maynard, A. *J. Phys. Chem. A* **1999**, *103*, 4572.

(13) Legon, A. C.; Aldrich, P. D.; Flygare, W. H. *J. Am. Chem. Soc.* **1982**, *104*, 1486.

(14) See, for example: Truscott, C. E.; Ault, B. S. *J. Phys. Chem.* **1984**, *88*, 2323.

(15) Hilfiker, M. A.; Mysak, E. R.; Samet, C. *J. Phys. Chem. A* **2001**, *105*, 3087.

(16) Wurrey, C. J.; Nease, A. B. *Vibrational Spectra and Structure: A Series of Advances*; Durig, J. R., Ed.; Elsevier: New York, 1978; Vol. 7. See Chapter 1.

(17) Streitwieser, A.; Caldwell, R. A.; Young, W. R. *J. Am. Chem. Soc.* **1969**, *91*, 529.

(18) Cram, D. J. *Fundamentals of Carbanion Chemistry;* Academic Press: New York, 1965.

(19) Bordwell, F. G.; Matthews, W. S. *J. Am. Chem. Soc.* **1974**, *96*, 1214.

(20) For a general review of hydrogen bonding, see: Jeffrey, G. A. *An Introduction to Hydrogen* Bonding; Oxford University Press: New York, 1997.

(21) See, for example: (a) Ault, B. S. *J. Am. Chem. Soc.* **1978**, *100*, 2426. (b) Dunkin, I. R. *Matrix Isolation Techniques: A Practical Approach*; Oxford University Press: New York, 1998.

(22) Frisch, M. J.; Trucks, G. W.; Schlegel, H. B.; Scuseria, G. E.; Robb, M. A.; Cheseman, J. R.; Zakrzewski, V. G.; Montgomery, J. A., Jr.; Stratmann, R. E.; Burant, J. C.; Dapprick, S.; Millam, J. M.; Daniels, A. D.; Kudin, K. N.; Strain, M. C.; Farkas, O.; Tomasi, J.; Barone, V.; Cossi, M.; Cammi, R.; Mennucci, B.; Pomelli, C.; Adamo, C.; Clifford, S.; Ochterski, J.; Petersson, G. A.; Ayala, P. Y.; Cui, Q.; Morokuma, K.; Malikk, D. K.; Rabuck, A. D.; Raghavachari, K.; Foresman, J. B.; Cioslowski, J.; Ortiz, J. V.; Stefanov, B. B.; Liu, G.; Liashenko, A.; Piskorz, P.; Komaromi, I.; Gomperts, R.; Martin, R. L.; Fox, D. J.; Keith, T.; Al-Laham, M. A.; Peng, C. Y.; Nanayakkara, A.; Gonzalez, C.; Challacombe, M.; Gill, P. M. W.; Johnson, B. G.; Chen, W.; Wong, M. W.; Andres, J. L.; Head-Gordon, M.; Replogle, E. S.; Pople, J. A. *Gaussian 98*, revision A.11.4; Gaussian Inc.: Pittsburgh, PA, 2002.

(23) (a) Becke, A. D. *Phys. Rev. A* **1988**, *38*, 3098. (b) Perdew, J. P.; Wang, Y. *Phys. Rev. B* **1992**, *45*, 13244.

(24) (a) Becke, A. D. *J. Chem. Phys.* **1993**, *98*, 5648. (b) Lee, C.; Yang, W.; Parr, R. G. *Phys. Rev. B* **1988**, *37*, 785.

(25) Petersson, G. A.; Bennett, A.; Tensfeldt, T. G.; Al-Laham, M. A.; Shirley, W. A.; Mantzaris, J. *J. Chem. Phys.* **1988**, *89*, 2193.

(26) Daly, L. H.; Wiberly, S. E. *J. Mol. Spectrosc.* **1958**, *2*, 177.

(27) Duncan, J. L.; McKean, D. C. *J. Mol. Spectrosc.* **1968**, *27*, 117.

(28) Duncan, J. L.; Burns, G. R. *J. Mol. Spectrosc.* **1969**, *30*, 253.

(29) Baker, A. W.; Lord, R. C. *J. Chem. Phys.* **1955**, *23*, 1636.

(30) Pimentel, G. C.; Bulanin, M. O.; Thiel, M. V. *J. Chem. Phys.* **1961**, *36*, 500.

(31) Goldfarb, T. D.; Khare, B. N. *J. Chem. Phys.* **1967**, *46*, 3379.

(32) Suzer, S.; Andrews, L. *J. Chem. Phys.* **1987**, *87*, 5131.

(33) Chaban, G. M. *J. Phys. Chem. A* **2004**, *108*, 4551.

(34) Carpenter, J. D.; Ault, B. S. *J. Phys. Chem.* **1991**, *95*, 3507.

(35) Yeh, Y. Y.; Wurrey, C. J. *J. Raman Spectrosc.* **1984**, *15*, 55.

(36) DeLaat, A. M.; Ault, B. S. *J. Am. Chem. Soc.* **1987**, *109*, 4232.

(37) Jeng, M. L. H.; DeLaat, A. M.; Ault, B. S. *J. Phys. Chem.* **1989**, *93*, 3997.

(38) Jeng, M. L. H.; Ault, B. S. *J. Phys. Chem.* **1989**, *93*, 5426.

(39) Jeng, M. L. H.; Ault, B. S. *J. Phys. Chem.* **1990**, *94*, 1323.

(40) Jeng, M. L. H.; Ault, B. S. *J. Phys. Chem.* **1990**, *94*, 4851.

(41) Ault, B. S.; Steinback, E.; Pimentel, G. C. *J. Phys. Chem.* **1975**, *79*, 615.

(42) Epley, T. D.; Drago, R. S. *J. Am. Chem. Soc.* **1967**, *89*, 5770.

(43) Allerhand, A.; Schelever, P. R. *J. Am. Chem. Soc.* **1963**, *85*, 866.

(44) Jain, S. C.; Riverst, R. *Can. J. Chem.* **1963**, *41*, 2130.

(45) Jain, S. C.; Riverst, R. *Inorg. Chem.* **1967**, *6*, 467.

(46) Farona, M. F.; Bremer, N. J. *J. Am. Chem. Soc.* **1966**, *88*, 3735.

(47) Coates, G. E.; Glockling, F. *Organometallic Chemistry*; Zeiss, H., Ed.; Reinhold: New York, 1960; p 461.

(48) Walton, R. A. *Q. Rev. (London)* **1965**, *19*, 126.

(49) Wetmore, S. D.; Schofield, R.; Smith, D. M.; Radom, L. *J. Phys. Chem. A* **2001**, *105*, 8718.

(50) See, for example: (a) Hehre, W. J.; Pople, J. A. *Tetrahedron Lett.* **1970**, *11*, 2959. (b) Tollenaere, J. P.; Moereels, H. *Tetrahedron Lett.* **1978**, *15*, 1347. (c) Baeten, A.; Proft, F. D.; Langenaeker, W.; Geerlings, P. *J. Mol. Struct.: THEOCHEM* **1994**, *306*, 203. (d) Umeyama, X.; Morokuma, K. *J. Am. Chem.* Soc. **1976**, *98*, 4400.

(51) Del Bene, J. E.; Jordan, M. J. T. *J. Mol. Struct. (THEOCHEM)* **2001**, *573*, 11.

(52) See, for example: (a) Iwasaki, A.; Fujii, A.; Watanabe, T.; Ebata, T.; Mikami, N. *J. Phys. Chem.* **1996**, *100*, 16053. (b) Abkowicz-Bienko, A.; Latajka, Z. *J. Phys. Chem. A* **2000**, *104*, 1004.

(53) Craddock, S.; Hinchliffe, A. *Matrix Isolation*; Cambridge University Press: New York, 1975.